FULL PAPER

Revisiting the Structure of Graphene Oxide for Preparing New-Style Graphene-Based Ultraviolet Absorbers

Wenhui He and *Lehui Lu**

Despite sustained effort over the years, the exploration of an effective strategy toward understanding the structure and properties of graphene oxide (GO) is still highly desirable. Herein, a facile route to revisit the structure of GO is demonstrated by elucidating its chemical-conversion process solely in the presence of ammonia. Such a strategy can contribute to settling some arguments in recent models of GO, and also offers a prerequisite to identify critical components that can act as ultraviolet absorbers (UVAs) in resulting dispersions of nitrogen-doped graphene sheets (NGSs). Inspired by this, for the first time, the performance of NGSs, serving as new-style UVAs, is investigated through directly assessing the effect of NGSs on the photofastness of azo dyes (Food Black). These studies reveal that, distinct from the common understanding, the as-prepared NGSs can dramatically enhance the photostability of Food Black under UV irradiation and exhibit greatly applied potential as a multifunctional UVA for new-generation inkjet inks that can simultaneously integrate the advantages of dye-based and pigment-based inks.

1. Introduction

Graphene sheets – one-atom-thick, 2D layers of sp^2-hybridized carbon – are now well known for their unique physical properties and potential applications in various fields.[1,2] Among all of the strategies pursued for producing graphene, the reduction of graphene oxide (GO) provides a promising route to large quantities of processible graphene at low cost.[1a,b] However, the precise chemical structure of GO, despite extensive investigation over the years, is still a subject of intense debate,[1b] which directly limits its controllable functionalization and blocks the way to understand its intrinsic characteristics, as well as its role in graphene-based composites. Because of this, interest in the structure of GO has never flagged.[3] Aside from two typical models of GO (i.e., the Lerf–Klinowski model[3a] and the Dékány model[3b]), Rourke's group[3d] has recently demonstrated the existence of highly oxidized debris (OD) on the surface of GO, clearly paving a new way to revisit the structure of GO. Nevertheless, restricted to the experimental process,[3d] it is difficult to obtain purified OD, the structure of which is anticipated to offer further valuable information to identify the probable GO model. Therefore, the exploration of an effective route to the structural analysis of the OD may achieve an expected breakthrough toward understanding the structure and properties of GO.

Ultraviolet absorbers (UVAs) are a class of functional fillers, used widely in industry, that can reduce the damaging effects of UV radiation on the properties of materials.[4] Classical inorganic UVAs, such as TiO_2, CeO_2, and ZnO, are preferable, partly due to their high stability and low cost,[5] but they are also well known as high-performance photocatalysts, which directly limits their application in certain fields involving organic dyes (i.e., dye-based inks), where organic UVAs are inevitably chosen instead.[6] Unfortunately, organic UVAs often need time-consuming processing and only absorb UV light of appointed wavelengths because of their specific molecular structure.[7] Thus, the facile synthesis of an alternative UVA is highly desirable. According to previous reports,[1a,8] reduced GO shows a strong UV–vis absorption at 230–400 nm, and also posesses extraordinary structural properties, including a large special surface area, and a unique 2D and π–π conjugated structure, all of which perfectly match with the desired properties of functional additives needed in dye-based inks.[9] However, to the best of our knowledge, a study of the usage of reduced GO as a UVA has not appeared in the literature yet, presumably owing to the relatively poor stability and complex composition of the resulting reduced GO dispersions, as well as the existing mindset that graphene is invariably related to the subject of photodegradation of dyes.

Distinct from common understanding, in this report, for the first time, we reveal the potential of nitrogen-doped graphene sheets (NGSs) to serve as an inexpensive, potent, and multifunctional UVA for dye-based ink. To set up a nice model system to evaluate the utility of reduced GO as a UVA, and ultimately to realize its application in dye-based ink, a facile strategy has been developed to synthesize reduced GO with two advanced features: i) excellent aqueous dispersibility, achieving the homogeneous mixing with the dyes; and ii) clean, reduced-GO sheets without foreign stabilizers and active reagents, helping to assess directly the effect of the reduced GO on the photostability of dyes. More importantly, we further unveil the reduction mechanism of GO in our system, which provides not only a new angle to revisit the structural model of GO, contributing to settling some arguments in recent models of GO, but

W. H. He, Prof. L. H. Lu
State Key Laboratory of Electroanalytical Chemistry
Changchun Institute of Applied Chemistry
Chinese Academy of Sciences
Changchun 130022, PR China
E-mail: lehuilu@ciac.jl.cn

DOI: 10.1002/adfm.201102998

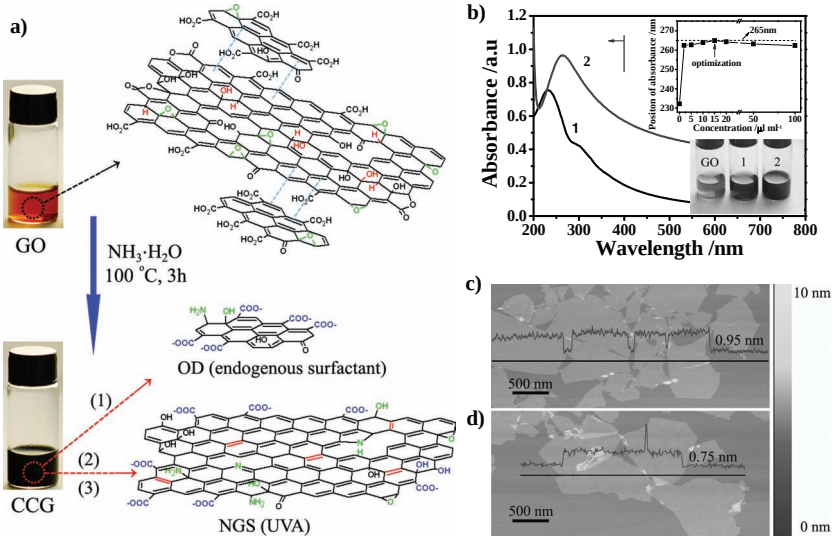

Figure 1. a) Scheme for the preparation of NGSs, and the reduction mechanism of GO: (1) removing OD from the graphene-like nanosheets; (2) dehydration to restore the aromatic structure; (3) incorporating nitrogen into the graphene-like sheets. b) UV–vis absorption of GO dispersions corresponding to different addition ratios of ammonia; inset: photographs of aqueous dispersions (≈0.5 mg mL^{-1}) of GO, after the treatment with ammonia (15 μL mL^{-1}) (2) or without ammonia (1). c–d) AFM images of GO (c) and CCG (d).

also a prerequisite to identify critical components that could serve as UVAs in resulting reduced-GO dispersions. Owing to the effect of nitrogen doping, the resultant NGSs exhibit some remarkable properties, including an improved work function and a decreased electrical conductivity, both of which, in combination with their significant UV-shielding effect, rationally explain the surprising improvement of the light-fastness of an azo dye under UV irradiation. Our results also highlight that the delicate tuning of the chemical and physical properties of GO may endow it with some new characteristics, even contrary to the common concepts, thus enabling the utility of GO and its derivatives in various new fields.

2. Results and Discussion

2.1. Synthesis and Characterization of NGSs

Chemically converted graphene (CCG) dispersions could be facilely synthesized by a hydrothermal treatment of GO in the presence of ammonia, as illustrated in **Figure 1**a. A notable color change from yellow-brown to dark indicated the reduction conversion of GO. In this system, the resulting reduction level of the CCG strongly relied on the concentration of ammonia, which could be readily monitored by UV–vis spectroscopy (Figure 1b). With an increasing concentration of ammonia (≈0–15 μL mL^{-1}), the absorption peak of the GO showed a significant red-shift from 230 nm to 265 nm (Figure S1a, Supporting Information), accompanied by a characteristic absorption enhancement in the whole spectral region (>230 nm), due to the restoration of the π-conjugated structure of graphene.[8a] The reaction did not proceed in the absence of ammonia (only a slight color change, Figure 1b, inset 1). By further exploring the effect of different addition ratios of ammonia (≈0–100 μL mL^{-1}) on this reaction (Figure 1b and Figure S1b), the optimal concentration of ammonia was fixed to 15 μL mL^{-1}, based on two nice characteristics: the maximum absorption at 200–400 nm and the excellent stability of the CCG dispersions, both of which well satisfied the fundamental requirements of a UVA. The CCG dispersions remained stable for several weeks in a sealed container, as further confirmed by the well-isolated sheets in the atomic force microscopy (AFM) images shown in Figure 1d. The average thickness of the CCG sheets was measured as 0.75 nm, typical for a single layer, which was smaller than that of well-exfoliated GO sheets (Figure 1c). This can be explained tentatively by the removal of oxygen-related groups within the GO sheets and the absence of any foreign stabilizers.

The excellent stability of the CCG dispersions made it difficult to concentrate the graphene sheets only by intensive centrifugation. To induce their aggregation, an appropriate amount of NaCl was added. Then, black aggregates were obtained by centrifugation, washed with distilled water, and dried under vacuum. To investigate the composition of the black aggregates further, X-ray photoelectron spectroscopy (XPS), and elemental analysis (EA) were employed. Compared with GO, the noticeable increase of the C/O ratio in the black aggregates could be identified easily from the survey-scan XPS spectra and EA (Figure S2 and Table S1), while the C 1s peaks[10] at 286.6 eV (hydroxyl) and 287.1 eV (epoxy) weakened dramatically (**Figure 2**a), indicating the removal of these oxygen-related groups. Moreover, a new peak at 285.8 eV corresponding to the C–N groups emerged,[10c,d] and the weight percentage of nitrogen was measured to be about 5% by EA, suggesting that these black aggregates were NGSs. Complementary to the XPS analysis and EA, the successful reduction of GO was also verified by Fourier transform IR (FTIR) spectroscopy and thermogravimetric analysis (TGA) of the NGSs (Figure 2b,c).

2.2. Insights into the Reduction Mechanism of GO

To unravel the details of this reaction, we analyzed the reduction process of the GO carefully. Indeed, some studies have demonstrated the synergistic effect of ammonia on the reduction of GO,[8a,11] but the real role of ammonia in these reactions has not been investigated yet. In this system, three new components (NH_3, OH^-, and NH_4^+) could be in coexistence in the resulting GO dispersions, due to the solubility and ionization of ammonia. Evidently, NH_3 and OH^- provided an alkaline environment and could serve as nucleophilic reagents,[3a] whilst NH_3 or NH_4^+, containing negative trivalent nitrogen, might act as reduction agents. However, considering the weak oxidative property of GO,[3d] we speculated

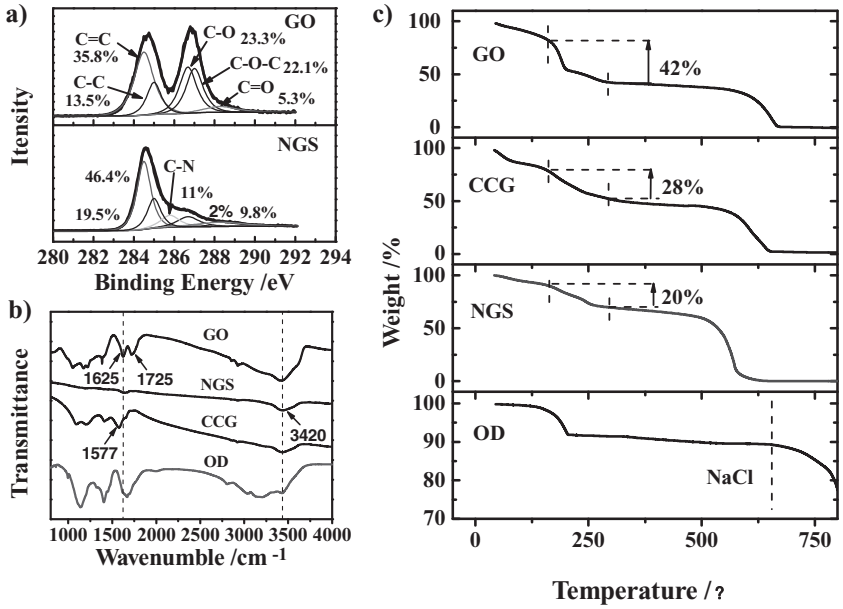

Figure 2. a) High-resolution C 1s spectra of GO and NGSs. b) FTIR absorption spectra of the as-produced GO, NGSs, CCG, and OD; the dashed gray lines mark the bands at around 1625 cm^{-1} and 3420 cm^{-1}. c) Thermogravimetric analysis in air of GO, NGSs, CCG, and OD.

that NH_3 or NH_4^+ couldn't be an effective reducing agent here. In this regard, the reduction of GO probably originated from the nucleophilic attack of NH_3 or OH^-, similar to the reduction of GO under alkaline conditions.[3a,12] In a recent study made by Rourke's group,[3d] GO was considered as a large, functionalized graphene-like sheet physically adsorbed with lots of small, highly oxidized debris (OD) that could be washed away under alkaline conditions. Thus, it was anticipated that similar components to the OD from the CCG dispersions could be extracted. After being separated from the black aggregates (NGSs) by centrifugation, the colorless supernatant was dried under vacuum to give a slightly yellow powder, and was further analyzed by FTIR spectroscopy and TGA. As shown in Figure 2b, similar to GO, the IR spectra of the yellow powder also illustrated the absorption bands of various oxygen-related groups, such as O–H (at ≈3403 and ≈ 1395 cm^{-1}), C–O (at 1060–1200 cm^{-1}), and C=O/COOH (at ≈1700 cm^{-1}), consistent with the results reported by Rourke' group.[3d] Moreover, the attenuated absorption band of C–O–C (at ≈1230 cm^{-1}) was also observed, which might be contributed by the preferential reaction of C–O–C with NH_3 or OH^- by nucleophilic attack.[3a,b] Additionally, TGA of the yellow powder showed a significant low-temperature mass loss at around 200 °C as a result of the decomposition of various oxygen-related groups,[13] while the residue (NaCl) kept stable until the temperature over-ran 600 °C (Figure 2c), suggesting that there were no components containing graphitic regions in the yellow powder.[3d] In view of these discussions, two obvious conclusions could be obtained: firstly, the OD really existed, partly supporting the structural model of GO given by Rourke's group;[3d] secondly, the high reduction level of the NGSs was mainly due to the effective removal of OD from the surface of the GO.

Currently, the several structural models of GO that are proposed are based mainly on the analysis of experimental data involving the whole of the graphene-like sheets and the OD.[1b,3] In contrast, the discovery of the OD has provided a new angle to revisit the structure of GO. Significantly, in this study, pure OD could be readily prepared by just modifying the concentrations of the GO and ammonia (details in the Experimental Section), and presented a yellow powder (**Figure 3**a, 2 in inset). AFM images of the OD revealed its relatively small size and a typical topographic height of 0.5–1.0 nm (Figure S3). Moreover, the composition of OD was further assessed by XPS and EA. As shown in Figure 3a, the C 1s spectrum of OD was deconvoluted into five peaks, which showed two distinct features in comparison with GO and NGSs. Firstly, the area of the peak at 284.5 eV, generally assigned to C=C,[10] reached as large as 45%, which was much larger than that of C–C (at 285.1 eV, 3%). This helped to interpret the strong interaction between the OD and the graphene-like sheets by π–π stacking. Moreover, the OD had a larger area percentage of COOH (at 288.7 eV),[10] potentially as large as 24.5%, so the origin of the observed acidity of GO can be explained easily. Evidently, the abundant surface charges and strong affinity by π–π stacking commended OD as an endogenous and effective surfactant, which also explains the excellent stability of the NGSs dispersions in our experiment. Additionally, the EA of the OD revealed a relatively higher oxidation level than that of GO (Table S1), implying its significant influence on finalizing the category and distribution of oxygen-related groups within the GO. Significantly, since XPS is a surface-analysis technique, the high oxidation level of GO detected by XPS can be largely ascribed to the absorbed OD. In this case, the high percentage of COOH groups within GO detected by XPS

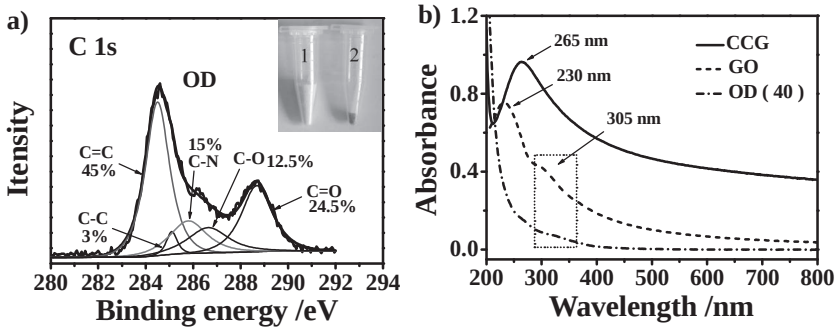

Figure 3. a) High-resolution C 1s spectrum of OD. Inset: photographs of OD mixing with NaCl (1) and without NaCl (2). b) UV–vis spectra of GO, CCG (with the addition of ammonia (15 μL mL^{-1})) and OD (concentrated to 40 times).

could be rational, which has been suspected previously and argued by other groups.[3b] Also, it suggests that the numerous carboxylic groups within the OD might be the real active sites for the chemical functionalization and the immobilization of functional nanoparticles on the surface of GO. Obviously, considering the presence of the OD, detailed functional groups within the graphene-like sheets require more careful studies.

Another unaddressed issue arose in as to whether the removal of OD is just a physical process or involves chemical conversion. As a physical process, it should be reversible. However, acidification didn't reverse the color change, except for inducing irreversible conglomeration (data not shown). Moreover, the excellent dispersibility of the CCG and the OD enabled their optical characters to be identified using UV–vis spectroscopy. As shown in Figure 3b, compared with GO, the OD showed an extremely weak UV–vis absorption in the whole spectral region (>220 nm), even after being concentrated to 40 times, indicating a lack of large π-conjugated graphitic regions within the OD, as proved above by TGA. Moreover, similar to GO, a weak characteristic absorption band at 305–320 nm was observed, further showing the high oxidation level of the OD.[14] Obviously, the presence of OD wouldn't shield the characteristic absorption of graphene-like sheets; that is, the red-shift of the absorption peak of the CCG dispersions mostly resulted from the NGSs. Thus, we inferred that the removal of OD from the graphene-like sheets could never be a physical process. As a proof of concept, CCG (a mixture of NGSs and OD), dried directly by freezing in a high vacuum, was assessed by FTIR spectroscopy and TGA. As shown in Figure 2b, the FTIR spectra of the CCG showed a new band at 1577 cm^{-1}, which is usually assigned to aromatic ν(C=C),[15] further confirming the restoration of the π-conjugated structure within the NGSs. TGA was used to identify the difference of the thermal stabilities between the GO and the CCG (Figure 2c). For the GO, there was a dramatic weight loss (≈42%) between 160 °C and 300 °C, whereas the CCG showed a lower weight loss (≈28%), implying a higher thermal stability and fewer oxygen-related groups of CCG.[13] Thus, the removal of oxygen-related groups within graphene-like sheets really occurred in our system. This might be attributable to a dehydration reaction driven by the need to restore the aromatic structure, similar to the mechanism proposed by Liao and coworkers,[16] so tertiary hydrogen should probably exist in the graphene-like sheets. Consequently, the underlying reduction mechanism of GO in this work is summarized in Figure 1a.

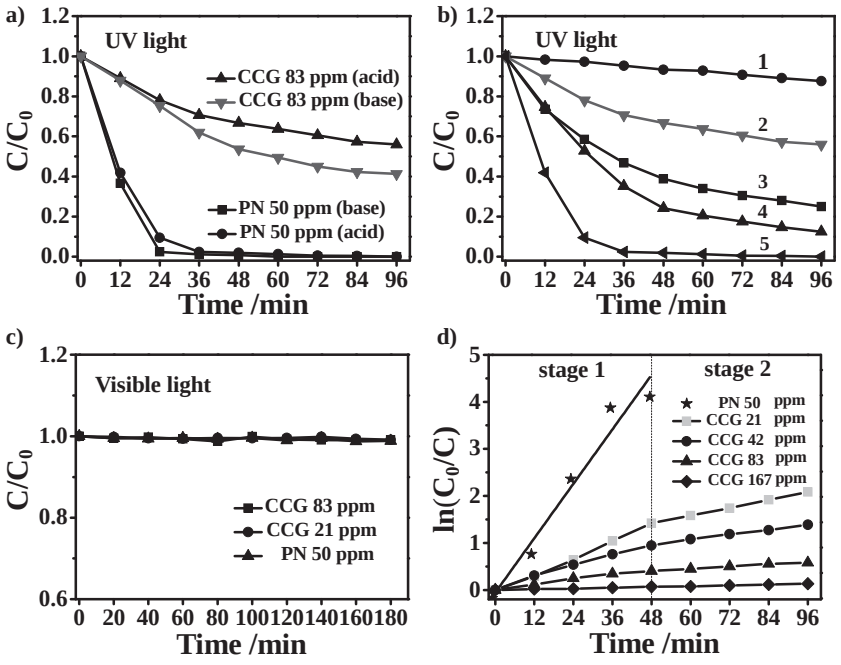

Figure 4. a) Normalized concentration of Food Black (PN) versus UV-irradiation time under different conditions; the initial concentration of Food Black was 50 ppm. b) Degradation of Food Black (PN) (50 ppm) under UV-light irradiation with various concentration of CCG: 167ppm (1);83 ppm(2); 42ppm (3);21 ppm (4); none (5). c) Normalized concentration of Food Black versus visible-light irradiation time under different conditions. d) $\ln(C_0/C)$ versus irradiation time (UV light) for Food Black with various concentrations of CCG.

2.3. Light-Fastness of Food Black under UV Irradiation with or without NGSs

Based on the above research, a clear difference between the characteristics of the OD and NGSs in the resulting CCG dispersions could be identified. Inspired by this, we further explored the effect of the NGSs on the photofastness of Food Black (a typical diazo dye used widely in the ink industry). Under UV irradiation, Food Black degraded gradually (Figure S5a), which can be explained by the intervention of singlet oxygen ($^1O_2$) that originated from the tautomeric (arylazo)-naphthols.[17] Considering the alkaline characteristics of NGSs dispersions, as well as the dependence of the interaction between the dyes and the NGSs on the pH value, the photostability of Food Black both in basic (pH = 10.0) and acid (pH = 4.0) conditions was also investigated (**Figure 4**a). The normalized temporal concentration changes (C/C_0) of the Food Black under UV irradiation were proportional to the normalized maximum absorbance (A/A_0) and derived from changes in the dye's absorption profile ($\lambda \approx$ 571 nm) at a given time interval. Interestingly, upon addition of ammonia, the photofading of Food Black proceeded rapidly and was nearly completed within 48 min. A similar phenomenon was also observed upon adding hydrochloric acid. This may be due to the inherently small HOMO-LUMO energy gap of Food Black, which results in its enhanced reactivity toward both nucleophiles and electrophiles.[18] Contrastingly, in the presence of NGSs, the initial dyes still remained at ≈60% and ≈40% in acid and basic solutions, respectively, after 96 min of UV irradiation (Figure 4a). Despite the similar photodegradation rate of pure Food Black both in acid and alkaline solutions, surprisingly, Food Black (mixed with NGSs) in acid conditions exhibited a higher stability than in basic conditions by approximately 20%. It was inferred that Food Black adsorbed on the surface of the NGSs could gain a better photostability (Figure S5b).

Additionally, the light-fastness of Food Black with various addition ratios of NGSs was also investigated. To enhance the interaction between the Food Black and the NGSs, all of the tests were performed in acid conditions (pH = 4.0). Obviously, on increasing the concentration of the NGSs, the light-fastness of the Food Black was significantly improved (Figure 4b). According to previous studies,[19] the degradation of dyes can be depicted by a simplified Langmuir–Hinshelwood model when C_0 is very small: $\ln(C_0/C) = k_a t$, where k_a is the apparent first-order rate constant. Similarly, it could describe the inhibiting effect of NGSs on the degradation of Food Black in our system, as displayed in Figure 4d. When the concentration of CCG reached 167 ppm, the degradation of Food Black (50 ppm) followed the pseudo-first-order kinetic model (PFKM) with a k_a value of 1.38×10^{-3} min^{-1}, which is far smaller than that of pure Food Black ($k_a = 8.11 \times 10^{-2}$ min^{-1}), indicating the powerful ability of NGSs to enhance the photostability of Food Black. However, for lower amounts of NGSs (concentration of CCG < 167 ppm), the degradation of Food Black diverged from the PFKM in the whole time range and formed an obvious division at 48 min, which can be described as a two-stage pseudo-first kinetic process.[19a] This unique dependence of the photodegradation rate of Food Black on the irradiation time can be explained by the different interactions between Food Black and the NGSs, which were largely impacted by the content of the NGSs. For a low concentration of NGSs, the dispersed dyes couldn't be adsorbed completely. Therefore, despite the presence of the UV-shielding effect of the NGSs, these isolated dyes also degraded gradually and even ran out within 48 min of UV irradiation in our experimental conditions. However, after 48 min of UV irradiation, the residual Food Black dye was that adsorbed by the NGSs, and thus a higher photostability and a smaller rate constant were obtained (details listed in Table S2).

What's more, it may be interesting to compare the anti-UV properties of NGSs and traditional UVAs. In previous studies, typical organic UVAs, such as benzophenones and benzotriazines, have been widely used to enhance the light-fastness of azo dyes.[20] In these cases, the UVA can absorb the harmful UV radiation preferentially and then dissipate the absorbed energy as benign heat by means of rapid tautomerism.[21] However, during the isomerization process, potential photodegradation of the UVA may also exist,[22] which directly results in the decrease of their anti-UV property (Figure S6). In comparison, the NGSs could keep a stable anti-UV property because of their excellent structure stability, and could also serve as multifunctional black pigments with the potential of improving the water-fastness of ink prints, as we will discuss below, thus showing greater applied potential in dye-based inks than traditional UVAs.

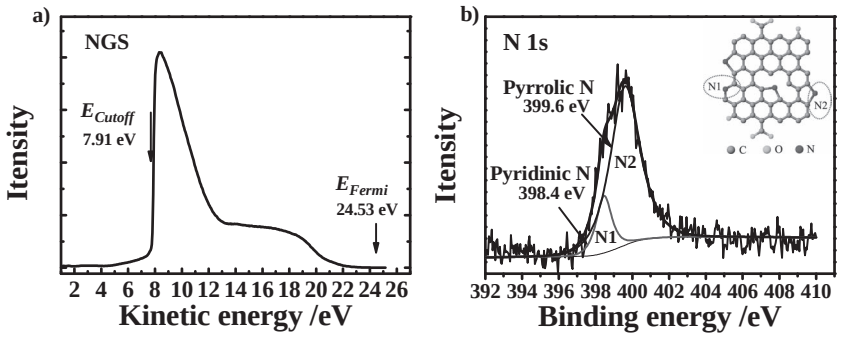

Figure 5. a) UPS spectrum of NGSs film. b) High-resolution N 1s XPS spectrum of NGSs.

2.4. Intrinsic Characteristics of NGSs

To better understand the improved photostability of Food Black under UV irradiation, two critical characteristics of NGSs need be considered. Firstly, owing to their intense absorption at 200–400 nm, NGSs can effectively filter out UV radiation. In this case, NGSs serves as a UVA. Secondly, with the NGS, the photosensitized degradation of Food Black is capable of being avoided, which was confirmed by the higher photostability of Food Black after being absorbed by the NGSs. However, to a certain extent, this conclusion seems to be in conflict with results reported by Zhao's group.[23] They found that the underlying electron transfer between reduced GO (reduced by $NaBH_4$) and an excited dye (Rhodamine B (RhB)) could induce an extremely slow degradation of the dye under visible-light irradiation.[23a] In this regard, the photostability of Food Black under visible-light irradiation was also investigated to exclude the influence of light sources (Figure 4c). Clearly, Food Black remained stable under visible-light irradiation no matter if NGSs were present or not. Also, the photostability of Food Black wasn't affected by the concentration of the NGS. This distinct conclusion might be attributed to the difference in preparation methods of reduced GO.

To gain an insight into the effect of the reduction conditions on the properties of reduced GO, we further prepared another two types of reduced GO using hydrazine and $NaBH_4$ as reducing agents: these two types of reduced GO were designated as HRGO and BRGO respectively. Ultraviolet photoelectron spectroscopy (UPS) was employed first, to measure the work functions of these three materials in ultrahigh vacuum. As shown in **Figure 5**a, the UPS spectra of the NGSs were recorded on the kinetic-energy scale. Subsequently, the work functions (W_F) were calculated by using the equation: $W_F = h\nu - D$,[24] where $h\nu$ is the photon energy and D is the spectrum width. Ultimately, the W_F of the NGSs was confirmed as 4.61 eV, while the W_F of the HRGO and BRGO corresponded to values of 4.7 eV and 4.36 eV respectively (Figure S10). Obviously, compared with the theoretical W_F of graphene (4.42 eV),[23a,25] the W_F of BRGO showed a smaller value, even smaller than that of TiO_2 (4.4 eV).[26] In contrast, the HRGO and the NGSs had a larger value of the W_F, which can be ascribed to the effect of nitrogen doping.[27] In addition, using the equation: E_{NHE} (V) = –4.5 + W_F,[23a,28] we found that the redox potential of BRGO versus a normal hydrogen electrode (NHE) was lower than that of TiO_2. This suggests that there was a larger potential difference between the BRGO and O_2 than between TiO_2 and O_2, thus leading to a larger driving force for producing various reactive oxygen species (ROS).[26] This explains the slight degradation of RhB (mixed with BRGO) under visible-light irradiation well, as observed by Zhao's group.[23] In contrast, the higher redox

Table 1. Electrical - conductivity data and work function (W_F) of GO, NGSs, HRGO, and BRGO.

	GO	**NGSs**	HRGO	BRGO
W [eV]	-	**4.61**	4.7	4.36
Electrical conductivity [S m^{-1}]	insulator	**4.5**	6859	119

potential of NGSs, closer to the potential of O_2, was expected to retard the formation of ROS, which partly explains the increased photostability of Food Black in our experiment.

However, it has been reported that incorporating nitrogen or boron into carbon materials can break their electroneutrality to create charged sites favorable for O_2 adsorption.[27,29] Thus, apart from effectively improving the W_F of graphene sheets, N doping may also render NGSs active, to induce the subsequent formation of ROS, which may promote the photodegradation of dyes. Fortunately, this phenomenon wasn't observed during our experimental process. To explain it, the N-bonding configurations in NGSs were further analyzed by way of their XPS spectra. As shown in Figure 5b, the complex N 1s spectra can be deconvoluted into two different signals corresponding to pyridinic N and pyrrolic N, respectively.[29,30] Due to the mildly doped condition,[30] graphitic N with a higher binding energy (≈401.3 eV) was not observed, while the content of pyridinic N was relatively low. According to recent reports, it has been suggested that the effective activation of O_2 depends heavily on the contents of pyridinic N and graphitic N in N-doped carbon materials.[31] Thus, we can conclude that the capability of NGSs of promoting the formation of ROS is relatively low. Moreover, the conductivity of the three materials was measured using the four-point-probe method, as listed in **Table 1**. Evidently, electron accumulation on the surface of the NGSs was anticipated to exist, due to their low conductivity. Considering the strong π–π interaction between the dyes and NGSs, this electron accumulation could further accelerate the recombination of electrons and oxidized dye radicals, ultimately suppressing the degradation of dyes. It also helps to explain the higher photostability of Food Black after being absorbed by NGSs, as depicted in **Figure 6**. Clearly, as discussed above, our results also highlight that the properties of reduced GO would be significantly impacted by its reduction route, which should be a valuable reference for designing and synthesizing novel graphene-based composites.

2.5. Application of NGSs in Dye-Based Ink

These favorable properties of NGSs inspired us to exploit their application in dye-based inks, where the poor light- and water-fastness of ink prints have always been big problems due to the use of disperse dyes as colorants.[32] Moreover, previous studies have proved that graphene-based patterns on various substrates can be prepared facilely by inkjet-printing,[33] which has expanded the potential of graphene in the ink industry greatly. To simulate the way of inkjet-printing, a solution of pure Food Black, or a mixture of CCG and Food Black, was smeared on a piece of paper (3.5 cm × 10 cm) drop by drop (inset in **Figure 7**a). After a prolonged UV irradiation, the residue of pure

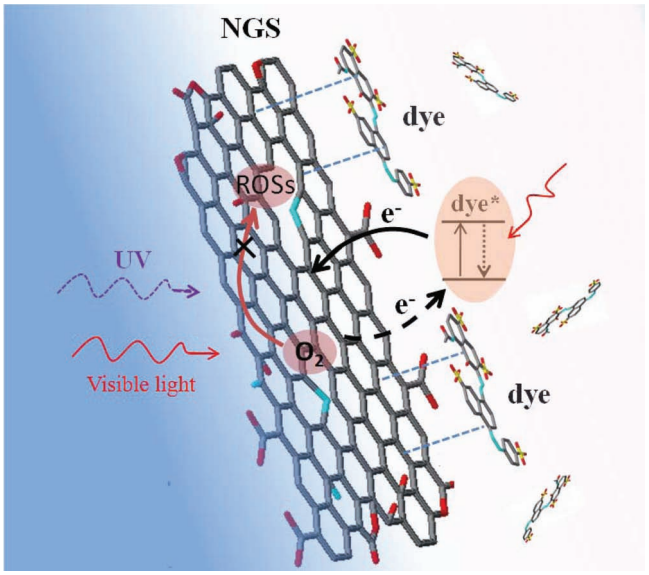

Figure 6. Mechanism for the enhanced photofastness of dyes (Food Black), mainly deriving from the UV shielding effect and the intrinsic characteristics of NGSs.

Food Black within the paper decreased gradually, as shown in Figure 7a. In contrast, in the presence of the NGSs, the degradation rate of the Food Black decreased noticeably, even down to zero after discontinuous exposure for 60 min. Clearly, the different diffusion properties between the Food Black and the NGSs to the paper should be responsible for the enhanced light-fastness of the Food Black. After being smeared, Food Black penetrated into the paper rapidly, owing to its smaller molecular scale, while the NGSs were left out of the paper and adsorbed strongly to form a protective layer (Figure 7f, g) that could filter out the UV radiation effectively. Meanwhile, as shown in Figure 7c,d, due to the strong π–π packing coupled with the unique 2D structure, the NGSs formed a smooth protective film against the paper, thus discarding the disadvantages of traditional inorganic pigments in pigment-based ink,[34] such as carbon black, and ultimately obtained a higher luster and chroma.

In addition, since the Food Black on the surface of the ink spots couldn't be protected by the NGSs, we further investigated the changes in the surface characteristics of the ink spots after exposure to UV irradiation for various times by assessing the surface wettability. As shown in Figure 7b, the ink spot of pure CCG had a strong hydrophobicity with a water contact angle of 85.5°. In contrast, the ink spots resulting from the mixture of CCG and Food Black had a smaller water contact angle than expected, due to the adsorption of Food Black on the surface by strong π–π interactions. However, after exposure to UV irradiation, the contact angle decreased gradually, which was contrary to our expectations. Generally, as the degradation of Food Black progressed, it was anticipated that it would display the surface characteristics of NGSs with a constant increase of water contact angle. This reverse phenomena can be explained by the adsorbed degradation products of Food Black, such as aromatic amines and aromatic carboxylic acids,[35] all of which helped to improve the hydrophilicity of the ink spots. Evidently, as a new multifunctional component,

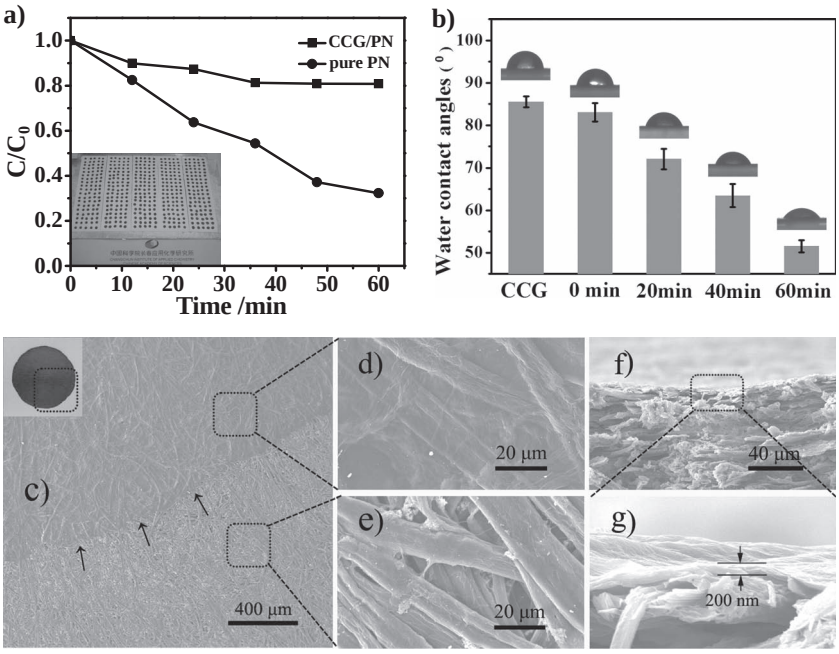

Figure 7. a) The residual concentration of Food Black (PN) in the scraps of paper versus UV-irradiation time; inset: photograph of the prints on the scraps of paper (3.5 cm × 10 cm × 5). b) Water contact angle of the ink dots (mixture of PN and NGSs) versus UV-irradiation time. c–g) SEM images showing the surface morphology of the ink dot (c), the thin film of NGSs (d) and the real surface morphology of the paper (e), and cross-sectional images of the ink dot (f) and the thickness of the NGSs film (g). The inset in Figure 7c shows a photograph of one of the ink dots (mixture of PN and NGSs).

NGSs can effectively improve the water-fastness of ink prints, and also inhibit the spread of the potentially toxic degradation products of dyes, while most traditional UVAs can't.

3. Conclusions

In summary, we have demonstrated a facile route to revisit the structure of GO by carefully analyzing the reduction process of GO solely in the presence of ammonia. Our results offer strong experimental evidence for the existence of OD, which can contribute to providing more information for the establishment of a new structural model for GO and as a valuable reference for creating novel graphene-based composites. Moreover, investigation into the reduction mechanism of GO allowed us to evaluate the great potential of NGSs as an efficient UVA to improve the light-fastness of azo dyes (Food Black). These studies not only shine light on the understanding of the direct interaction between dyes and reduced GO, but also open a new avenue toward new-generation inkjet inks that can integrate the advantages of dye-based and pigment-based inks effectively.

4. Experimental Section

Preparation of CCG: The graphene oxide (GO) was synthesized via a modified Hummers' method.[8b,36] Then, a suspension of the GO (0.5 mg mL^{-1}) was obtained by dispersing the graphene oxide in deionized (DI) water with the aid of ultrasonication for 30 min (500 W, 30% amplitude). In a typical procedure, GO (20.0 mL) was mixed with various amounts of ammonia solution (28–30 wt% in water) in a 30 mL glass vial, varying from 2 μL mL^{-1} to 500 μL mL^{-1} (the relative volume ratio between the ammonia and the GO dispersions). For comparison, DI water was further added to ensure that the resultant concentration of GO was the same in all of the cases mentioned above. After being stirred for a few minutes, the mixture was transferred into a polytetrafluoroethylene (PTFE) (Teflon) lined stainless-steel autoclave (50 mL), and treated at 100 °C for 3 h. After cooling down to room temperature, the back dispersions (CCG) were induced to aggregate by adding 20 mg of solid NaCl. A black aggregate was obtained by centrifugation (10 000 rpm, 30 min) and dried in vacuum to obtain a black powder (NGSs), while the colorless supernatant liquid was dried to give a light-yellow powder (OD mixed with NaCl). In addition, the CCG dispersions were dried directly by freezing in a high vacuum.

Preparation of Pure OD: The procedure for the preparation of pure OD was similar to that of CCG. Briefly, 30 mL of GO (1 mg mL^{-1}) was mixed with 1.2 mL of ammonia under stirring, then transferred into a Teflon lined stainless-steel autoclave (50 mL), and treated at 100 °C for 3 h. Due to the high concentration of GO and ammonia, the mixture was seriously aggregated. After intensive centrifugation (10 000 rpm, 30 min), the colorless supernatant was dried to give a yellow powder (OD).

Light-Fastness of Food Black on Real Paper with or without NGSs: In a typical procedure, several slips of paper with a size of 3.5 cm × 10 cm were firstly cut out. An aqueous solution of Food Black (800 ppm), as well as a mixture of Food Black (800 ppm) and CCG (500 ppm), was prepared. In order to imitate the way of inkjet printing, the aqueous solution of Food Black (or the mixture) was smeared on the paper slips drop by drop, with volumes of 5 μL, which resulted in the formation of 2D arrays (5 × 20). Subsequently, they were dried in an oven (80 °C). At given time intervals (5 min), six slips of the paper were exposed to the UV light, and then one of the paper slips was taken out every 10 min. Note that DI water, just a little, was sprayed on the paper slips before every exposure to the UV light to avoid a time-consuming UV irradiation. Subsequently, the paper slips were immersed in DI water (10 mL) for 12 h. After another sonication for 10 min, the supernatant solution was obtained by centrifugation, corresponding to the residue of Food Black in the paper, and was analyzed further by UV–vis spectroscopy. In the test of water contact angles, ink spots were prepared by dropping the mixture (150 μL) on a slip of paper. After drying in an oven (80 °C), the ink spots were exposed to UV radiation following a similar procedure as that for the paper slips. Subsequently, the surface characteristics of the ink spots were analyzed using a drop-shape analysis system.

Supporting Information

Supporting Information is available from the Wiley Online Library or from the author.

Acknowledgements

Financial support by the National Basic Research Program of China (973 Program; No. 2010CB933600), NSFC (No. 21125521) and the "Hundred Talents Project" of the Chinese Academy of Sciences is gratefully acknowledged.

Received: December 12, 2011
Revised: January 16, 2012
Published online: March 29, 2012

[1] a) S. Park, R. S. Ruoff, *Nat. Nanotechnol.* **2009**, *4*, 217; b) D. R. Dreyer, S. Park, C. W. Bielawski, R. S. Ruoff, *Chem. Soc. Rev.* **2010**, *39*, 228; c) S. Stankovich, D. A. Dikin, G. H. B. Dommett, K. M. Kohlhaas, E. J. Zimney, E. A. Stach, R. D. Piner, S. B. T. Nguyen, R. S. Ruoff, *Nature* **2006**, *442*, 282.

[2] a) H. Bai, C. Li, G. Q. Shi, *Adv. Mater.* **2011**, *23*, 1089; b) L. L. Li, K. P. Liu, G. H. Yang, C. M. Wang, J. R. Zhang, J. J. Zhu, *Adv. Funct. Mater.* **2011**, *21*, 1; c) Z. Liu, J. T. Robinson, X. S. Sun, H. J. Dai, *J. Am. Chem. Soc.* **2008**, *130*, 10876; d)H. Zhang, X. J. Lv, Y. M. Li, Y. Wang, J. H. Li, *ACS Nano* **2010**, *4*, 380; e) S. J. Guo, S. J. Dong, E. K. Wang, *ACS Nano* **2010**, *4*, 547.

[3] a) A. Lerf, H. He, M. Forster, J. Klinowski, *J. Phys. Chem. B* **1998**, *102*, 4477; b) T. Szabó, O Berkesi, P. Forgó, K. Josepovits, Y. Sanakis, D. Petridis, I. Dékány, *Chem. Mater.* **2006**, *18*, 2740; c) W. Gao, L. B. Alemany, L. J. Ci, P. M. Ajayan, *Nature Chem.* **2009**, *1*, 403; d) J. P. Rourke, P. A. Pandey, J. J. Moore, M. Bates, I. A. Kinloch, R. J. Young, N. R. Wilson, *Angew. Chem. Int. Ed.* **2011**, *50*, 3137; e) W. W. Cai, R. D. Piner, F. J. Stadermann, S. Park, M. A. Shaibat, Y. Ishii, D. X. Yang, A. Velamakanni, S. J. An, M. Stoller, J. An, D. M. Chen, R. S. Ruoff, *Science* **2008**, *321*, 1815; f) R. Larciprete, S. Fabris, T. Sun, P. Lacovig, A. Baraldi, S. Lizzit, *J. Am. Chem. Soc.* **2011**, *133*, 17315.

[4] M. Zayat, P. Garcia-Parejo, D. Levy, *Chem. Soc. Rev.* **2007**, *36*, 1270.

[5] a) D. Kundu, R. Mukherjee, *J. Mater. Sci. Lett.* **2003**, *22*, 1647; b) H. Sakamoto, J. Qiu, A. Makishima, *Sci. Technol. Adv. Mater.* **2003**, *4*, 69; c) O. K. Park, Y. S. Kang, *Colloids Surf. A* **2005**, *261*, 257.

[6] a) A. Lavery, J. Provost, *Recent Progress* in Ink *Jet Technologies II* (Eds.: E. Hanson, R. Eschbach), IS&T, Springfield, VA **1999**, pp. 400–405; b) W. J. Wnek, M. A. Andreottola, P. F. Doll, S. M Kelly, *Handbook of Imaging Materials*, 2nd revised ed. (Eds.: A. S. Diamond, D. S. Weiss), Marcel Dekker, New York **2002**, pp. 531–602.

[7] a) O. Hironori, *Dyes Pigments* **2001**, *48*, 151; b) B. Mahltig, H. Böttcher, K. Rauch, U. Dieckmann, R. Nitsche, T. Fritz, *Thin Solid Films* **2005**, *485*, 108.

[8] a) D. Li, M. B. Müller, S. Gilje, R. B. Kaner, G. G. Wallace, *Nature Nanotechnol.* **2008**, *3*, 101; b) Y. X. Xu, H. Bai, G. W. Lu, C. Li, G. Q. Shi, *J. Am. Chem. Soc.* **2008**, *130*, 5856; c) H. M. Sun, L. Y. Cao, L. H. Lu, *Nano Res.* **2011**, *4*, 550.

[9] a) J. Kettle, T. Lamminmäki, P. A. Gane, *Surf. Coat. Technol.* **2010**, *204*, 2103; b) T. T. Lamminmäki, J. P. Kettle, P. J. T. Puukko, P. A. C. Gane, *Ind. Eng. Chem. Res.* **2011**, *50*, 3287.

[10] a) J. F. Moudler, W. F. Stickle, P. E. Sobol, K. D. Bomben, *Handbook of X-ray Photoelectron Spectroscopy*, Perkin–Elmer, Eden Prairie USA **1992**; b) H. J. Shin, K. K. Kim, A. Benayad, S. M. Yoon, H. K. Park, I. S. Jung, M. H. Jin, H. K. Jeong, J. M. Kim, J. Y. Choi, Y. H. Lee, *Adv. Funct. Mater.* **2009**, *19*, 1987; c) S. Dubin, S. Gilje, K. Wang, V. C. Tung, K. Cha, A. S. Hall, J. Farrar, R. Varshneya, Y. Yang, R. B. Kaner, *ACS Nano* **2010**, *4*, 3845; d) J. Q. Liu, Z. Q. Lin, T. J. Liu, Z. Y. Yin, X. Z. Zhou, S. F. Chen, L. H. Xie, F. Boey, H. Zhang, W. Huang, *Small* **2010**, *6*, 1536.

[11] C. Z. Zhu, S. J. Guo, Y. X. Fang, S. J. Dong, *ACS Nano* **2011**, *4*, 2429.

[12] X. B. Fan, W. C. Peng, Y. Li, X. Y. Li, S. L. Wang, G. L. Zhang, F. B. Zhang, *Adv. Mater.* **2008**, *20*, 4490.

[13] H. K. Jeong, Y. P. Lee, M. H. Jin, E. S. Kim, J. J. Bae, Y. H. Lee, *Chem. Phys. Lett.* **2009**, *470*, 255.

[14] a) J. I. Paredes, S. Villar-Rodil, A. Martinez-Alonso, J. M. D. Tascon, *Langmuir* **2008**, *24*, 10560; b) V. Abdelsayed, S. Moussa, H. M. Hassan, H. S. Aluri, M. M. Collinson, M. S. El-Shall, *J. Phys. Chem. Lett.* **2010**, *1*, 2804.

[15] C. D. Zangmeister, *Chem. Mater.* **2010**, *22*, 5625.

[16] K. H. Liao, A. Mittal, S. Bose, C. Leighton, K. A. Mkhoyan, C. W. Macosko, *ACS Nano* **2011**, *5*, 1253.

[17] a) N. Kuramoto, T. Kitao, *J. Soc. Dyers Colour.* **1982**, *98*, 334; b) P. Bortolus, S. Monti, *J. Org. Chem.* **1989**, *54*, 534.

[18] E. Arunkumar, C. C. Forbes, B. D. Smith, *Eur. J. Org. Chem.* **2005**, *2005*, 4051.

[19] a) X. H. Wang, J. G. Li, H. Kamiyama, Y. Moriyoshi, T. Ishigaki, *J. Phys. Chem. B* **2006**, *110*, 6804; b) Y. J. Xu, Y. B. Zhuang, X. Z. Fu, *J. Phys. Chem. C* **2010**, *114*, 2669.

[20] A. H. Kehayoglou, E. G. Tsatsaroni, I. C. Eleftheriadis, K. C. Loufakis, L. E. Kyriazis, *Dyes Pigments.* **1997**, *34*, 207.

[21] a) J. E. A. Otterstedt, *J. Chem. Phys.* **1973**, *58*, 5716; b) M. Wiechmann, H. Port, F. Laermer, W. Frey, T. Elsaesser, *Chem. Phys. Lett.* **1990**, *165*, 28.

[22] a) J. Catalán, J. C. D. Valle, F. Fabero, N. A. Garcia, *Photochem. Photobiol.* **1995**, *61*, 118; b) J. Q. Pan, W. W. Y. Lau, Z. F. Zhang, X. Z. Hu, *Polym. Degrad. Stab.* **1996**, *53*, 153.

[23] a) Z. Xiong, L. L. Zhang, J. Ma, X. S. Zhao, *Chem. Commun.* **2010**, 6099; b) Z. Xiong, L. L. Zhang, X. S. Zhao, *Chem. Eur. J.* **2011**, *17*, 2428.

[24] a) Y. Park, V. Choong, Y. Gao, B. R. Hsieh, C. W. Tang, *Appl. Phys. Lett.* **1996**, *68*, 2699; b) X. C. Wu, Y. R. Tao, Q. X. Gao, *Nano Res.* **2009**, *2*, 558.

[25] X. Wang, L. J. Zhi, K. Mullen, *Nano Lett.* **2007**, *8*, 323.

[26] A. Hagfeldt, M. Graetzel, *Chem. Rev.* **1995**, *95*, 49.

[27] W. Yang, T. P. Fellinger, M. Antonietti, *J. Am. Chem. Soc.* **2010**, *133*, 206.

[28] M. Sadeghi, W. Liu, T. G. Zhang, P. Stavropoulos, B. Levy, *J. Phys. Chem.* **1996**, *100*, 19466.

[29] a) L. J. Yang, S. J. Jiang, Y. Zhao, L. Zhu, S. Chen, X. Z. Wang, Q. Wu, J. Ma, Y. W. Ma, Z. Hu, *Angew. Chem. Int. Ed.* **2011**, *50*, 7132; b) L. T. Qu, Y. Liu, J. B. Baek, L. M. Dai, *ACS Nano* **2010**, *4*, 1321.

[30] X. L. Li, H. L. Wang, J. T. Robinson, H. Sanchez, G. Diankov, H. G. Dai, *J. Am. Chem. Soc.* **2009**, *131*, 15939.

[31] S. B. Yang, X. L. Feng, X. C. Wang, K. Müllen, *Angew. Chem. Int. Ed.* **2011**, *50*, 5339.

[32] R. Steiger, P. A. Brugger, *Recent Progress* in Ink *Jet Technologies II* (Eds.: E. Hanson, R. Eschbach), IS&T, Springfield, VA **1999**, pp. 321–324.

[33] a) V. Dua, S. P. Surwade, S. Ammu, S. R. Agnihotra, S. Jain, K. E. Roberts, S. Park, R. S. Ruoff, S. K. Manohar, *Angew. Chem. Int. Ed.* **2010**, *49*, 2154; b) K. Y. Shin, J. Y. Hong, J. Jang, *Adv. Mater.* **2011**, *23*, 2113.

[34] a) C. Yoon, J. H. Choi, *Color. Technol.* **2008**, *124*, 355; b) C. Yoon, J. H. Choi, *Color. Technol.* **2011**, *127*, 186.

[35] a) L. C. Abbott, S. N. Batchelor, J. R. L. Smith, J. N. Moore, *J. Phys. Chem. A* **2009**, *113*, 6091; b) N. Kuramoto, T. Kitao, *J. Soc. Dyers Colour.* **1982**, *98*, 334.

[36] W. S. Hummers, R. E. Offeman, *J. Am. Chem. Soc.* **1958**, *80*, 1339.